ISBN: 978-3-95450-223-3 ISSN: 2673-7000 doi:10.18429/JACoW-NAPAC2019-WEPLO18

NUMERICAL STUDY OF COHERENT RADIATION FROM INDUCED PLASMA DIPOLE OSCILLATION BY DETUNED LASER PULSES

P.C. Castillo†, S.D. Rodriguez, D.A. Wan,
SUNY-Farmingdale State College, Farmingdale, NY, USA
K. Yu, Brookhaven National Laboratory, Upton, NY, USA
B. Gross, The City College of New York, NY, USA
D.G. Lee, Stony Brook University, New York, NY, USA
M.S. Hur, S. Kylychbekov, H.S. Song,
Uslan National Institute of Science and Technology, Ulsan, South Korea

Abstract

This research focuses on numerical studies and simulation of interacting counter propagating high-intense short laser pulses inducing strong oscillating dipoles in preformed plasma resulting in novel THz sources. By choosing a suitable frequency detuned colliding laser pulses, a cylindrical spatial plasma column will be established within the laser beam radius regime resulting in a time varying longitudinal ponderomotive field that can drive the charges coherently resulting in the formation of a stable spatially localized plasma dipole oscillation (PDO). This novel excitation approach can then result in emission of terahertz radiation transverse to the laser optic axis. While the general qualitative behavior of the 'released dipole' radiation can be easily modelled as a driven harmonic oscillator, the detailed microphysics during the dipole growth stage requires first principles modelling of the Radiation / Plasma system which can only be accomplished by our proposed 3D Particle in Cell (PIC) time dependent Partial Differential Equation steppers that evolve the simultaneous motions of the plasma charges and the EM fields. In this paper, we focus on a case where the emission is expected to be efficient and use the full 3D capabilities of our simulation environment to observe the radiation structure transverse to the laser induced dipole fields.

INTRODUCTION

The study of intense laser-plasma interactions is an active and growing field of both theoretical and applied research encompassing a variety of disciplines. As discussed in Kwon et. al. [1], there is strong interest in developing potential tunable compact high power-narrow band radiation sources that can be used for a number of applications. Most approaches to the generation of such sources are either expensive and physically large (i.e. Free Electron Lasers) [2-5] or low energy due to material breakdown limits [6]. In addition, the complex nonlinear time varying processes that may be encountered in the interaction of laser irradiation and high concentration plasma make analytical modelling difficult and approximate, and most fundamental studies require sophisticated numerical modelling approaches to account for the complex interactions that charged particle carriers can have with intense EM pulses that can further be focused onto spatial targets [7-9].

† castilp@farmingdale.edu

This research focuses on developing a suitable computational environment to simulate dense plasma effects during its interaction with high intensity lasers that can be manipulated to provide different laser interaction geometries.

In this paper, we focus on demonstrating through PIC simulations (x-y-z-t) recently discussed spatially modulated plasma dipole oscillation [1, 7, 10-16] induced by detuned counter-propagating laser pulses. Based on approximate 1D modelling and 1D and 2D PIC simulations, such an excitation process can generate a narrow band THz radiation at the Plasma Frequency [17-23]. Because of the high density of particles within the wavelength of the exciting pulses, the abovementioned physical processes require extensive computational simulations in order to process a large amount of data to represent the plasma density (millions of particles) within the Particle-in Cell system. Unlike most previous studies where either 1D or 2D PIC simulations are used, potentially interesting features of the EM-Laser interactions due to cylindrical 3D spatial geometries of the laser beam regime is investigated.

METHODS AND ALGORITHMS

In this numerical study, we adapted the Particle-In-Cell (PIC) method, which is implemented by a code named SPACE. Space is a relativistic and full 3D electromagnetic PIC (EM-PIC) code based on the finite difference time domain (FDTD) [24] being developed at Brookhaven National Laboratory (BNL) [25, 26]. Space has been verified and validated in the studies of a variety of beam-plasma and laser-plasma interaction scenarios such as HPRF at Fermilab [27, 28], CeC at BNL [29, 30], and LWFA at BNL [31, 32].

LASER/PLASMA SYSTEM SETTINGS

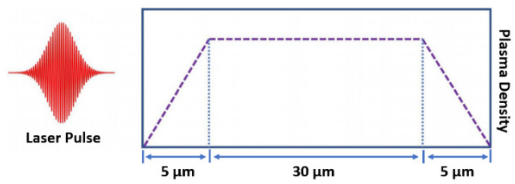

Figure 1: Schematic diagram of the laser pulse and plasma density profile along the pulse propagation direction. The preformed plasma has cilindrical shape of 40 μm length and 5 μm radius. The plasma density ramp up linearly from the both edges and the center part has constant density.

ISBN: 978-3-95450-223-3 ISSN: 2673-7000 doi:10.18429/JACoW-NAPAC2019-WEPLO18

In order to elucidate the laser-plasma interaction, the longitudinal counter propagation of two detuned short laser sources along the preformed plasma was simulated using the SPACE code. The parameters used in the laser / plasma system includes the wavelenght of the lasers as 0.800001μm and 0.760007μm with a normalize field amplitude (a_o) of 0.6.

We setup a 3D cubical spatial domain of 48μm simulation length, corresponding to a theoretical beam propagation time from side to side of 160fs. Within this domain, the first and last 4μm are set as vacuum, followed by the actual geometry of the plasma column, which has a trapezoidal shape corresponding to a linear ramp-up/down behaviour of 5μm for the incoming (left side) and outgoing (right side) travelling beam, and a flat volumetric region of 30μm length of effective plasma channel as in Fig. 1.

Specifically, the vacuum and linear ramp model are established in the domain since first, the system has no physical boundaries, and second, when simulating the interaction volume, we use a gradually linearly increasing tapered edge to reduce any reflection artifacts that will occur when outgoing radiation modes are propagated from the induced plasma dipole sources. Therefore any reflection is considered numerical noise and not due to physical boundaries, which are undesired and unphysical.

Figure 2A shows the counter-propagating laser pulses parallel to the z-axis. Both laser's beam profiles include a beam waist radius of 5μm and beam duration of 30fs. Gaussian profile short beams with 5μm radius allows the formation of a cylindrical channel within the total plasma domain, and therefore the main slab to account for laser-plasma interaction. In addition, the numerical setting for the plasma channel is modeled in a grid domain to account for the number plasma density of 4.97×10^{18} cm^{-3} as in [1].

RESULTS AND ANALYSIS

In illustrating the induced radiation patterns, it is crucial to focus not on the laser pulses themselves but the resultant ponderomotive forces and space-time development of the longitudinal electric fields of the plasma charge distributions. Because of the dynamics of the plasma interactions, the plasma response is not instantaneous and induced fields will not propagate at the same velocity of the actual pulses. In Fig. 2A, we plot the spatial (x-z) beam counter propagation, where the laser axis is at x=0. Figure 2B shows the E field intensity at the center of the plasma channel versus the physical time depicting the dynamics of the dipole induced field.

In particular, point 1 at Fig. 2B, shows that the initial interaction of the induced fields occurs at about 80fs, (blueish line potentials envelopes surrounding the induced fields at 24μm in Fig. 2A). The length of the induced fields are also about 24μm. Figure 2C depicts the overlap of the induced field tracers between 12μm and 36μm (24μm length) after each tracer travels 12μm from the initial interaction. The overlap of the fields occurs at 140fs (point A at Fig. 2B), resulting in the highest E field intensity during the collision, which defines the presence of the plasma dipole. Since the travelling distance from the initial interaction (point 1 at 80 fs) to the formation of the dipole (point A at 140fs) is about 12μm, and considering the time difference (60fs), we determined the effective velocity of the induced fields as 2×10^8 m/s. These results suggest that the plasma dipole is generated by the induced fields following the short pulses and not by the actual optical pulses.

In addition, we observed in Fig. 2B that the dipole electric field generally increases over time during the formation stage, reaching a peak value of about 20 GV/m. During this stage, we observed the formation of micro-bunches of trapped electrons from the induced charge distribution as shown in Fig. 3A (at 140fs) but unlike the 1D depictions of the ion bunching in [1], we observe the full 3D dynamics including transverse bulging at the collision center as well as a clustering of micro-bunches to form a single coherently formed super bunch. Consequently, after the pulses seperate and the restoring force of the dipoles again dominates the induced pondermotive forces, the dipole blocks release their energy as an underdamped oscillation decay at the plasma frequency, as shown in Fig. 3B (at 170fs) and 3C (at 250fs).

The full use of the 3D simulation environment is illustrated by the induced field patterns that are transversal to the optical axis. The build-up and emitted transverse radiation due the induced plasma dipole for different interaction times is shown in Fig. 4. Fig. 4A, shows the transversal profile of the initial stage of the laser's induced fields's interaction corresponding to the same longitudinal time frame shown in Fig. 2A, occurring at the same tracer's propagation time of 80fs as shown in the point 1 of Fig. 2B. The oscillation-relaxation that results in the transversal radiation modes is observed in Fig. 4C and can be matched with the charge behavior shown in Fig. 3B and 3C.

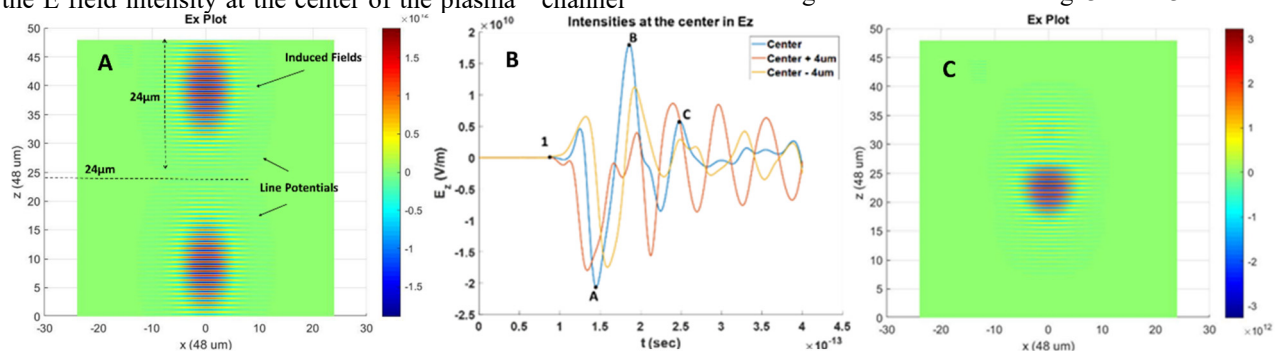

Figure 2: A) On-axis (x=0) transverse induced fields prior to collision. B) Electric field as a function of propagation time along the longitudinal axis. C) Axial view of the plasma dipole formation during the laser's induced field collision.

ISBN: 978-3-95450-223-3 ISSN: 2673-7000 doi:10.18429/JACoW-NAPAC2019-WEPLO18

Figure 4B shows the transversal view of the dipole during the overlapping of the induced fields corresponding to the same time frame of the longitudinal view shown in Fig. 2C, occurring at the same tracer's propagation time of 140fs as in point A of Fig. 2B. This can be also related to the micro-bunch charge distribution shown at Fig. 3A.

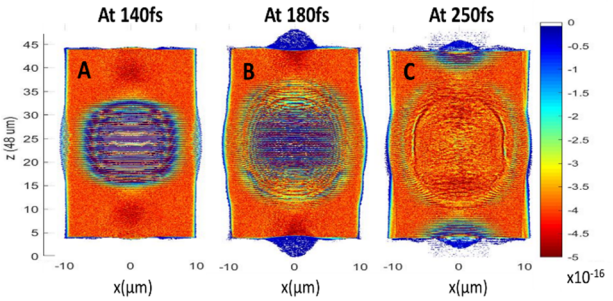

Figure 3: A) Micro-bunch of trapped electrons at the laser collision center. B) Micro-bunch distribution at the initial peak of the oscillation-relaxation at the plasma frequency. C) Single bunch formation probed at point C in Fig. 2A.

Most importantly, Fig. 4C clearly depict the general behavior of the laser-plasma interaction including the dipole formation, the diameter of the laser spot (10μm), the diffraction pattern of the Gaussian laser beam profile (Airy disk) resulting on inhomogeneous plasma densities, and most relevant, the radial emitted radiation from the interaction. Perhaps most surprisingly, from the time difference between point B and C (Period (ΔT) = $T_C - T_B$ = 70fs) in the oscillation relaxation region in Fig. 2B, we deduced the actual wavelength radiation (λ_{RAD} = c(ΔT), c =speed of light) to be 21μm, therefore the radiation frequency (f_{RAD}) equal to 14.3THz, which is significiantly below the Plasma Frequency (f_p=20THz) given by the set plasma density (n_e =4.97x10^{18} cm^{-3}) and $f_p = \frac{1}{2\pi}\sqrt{\frac{4\pi n_e e^2}{m_e^*}}$. This contradicts the fact that propagation of EM radiation can only occur for frequencies above the plasma frequency($f_{RAD} > f_p$). This unforeseen effect may be due to the concentration of high charge density distribution during the plasma dipole formation and post oscillation-relaxation (Fig. 3) within the spatial regime of the laser beam radius and Gaussian profile, which may cause plasma inhomogeneities with high densities in the center collision and lower densities outwards, which will result on a thicker filament between the unexcited background plasma and vacuum, causing some energy loss due to absorption and therefore a reduced transverse PDO radiation. In addition, intense short pulses undergoing spatial diffraction, dispersion and nonlinear interactions can lead to pulse breakup filamentation and other potential degradation issues, which should be studied in more detail.

CONCLUSIONS

In this paper, we present a preliminary analysis of the Embedded Dipole Oscilatton mechanism for counter propogating detuned lasers using full 3D PIC simuation capabilities. In an approximate 1D model, the laser pulse collision results in a drifting standing wave pattern that can efficiently induce large scale ion bunches to coherently radiate over the spatial cross-section of the interaction range. While the 1D model can estimate the boundaries of the processes, the detailed dynamics of the charge distributions requires a full 3D treatment. During the build-up phase when both laser fields are overlapping in a complex way, the spatial charge density patterns can be very disorganized, complex and nonsymmetrical, leading to messy incoherent movement and messy broadband radiation bursts. However, like in the 1D theory, once the counter propagating laser pulses pass through the preformed plasma, the effective macroscopic dipoles (space charge separations) can now freely and coherently relax and oscillate resulting in a robust transverse narrowband emitter

In the future, we will explore the injection of laser pulses to induce background plasma driven by the self-guided laser wakefield mechanism, which is used to perturb the plasma for induced dipole oscillations followed by radiation. Inducing a cylindrical spatial plasma column within the laser beam radius regime, it is expected that a stable spatially localized plasma channel will result and the emitted radiation from the plasma dipole oscillation (PDO) will not be affected by surrounding absorption, resulting in efficient coherent radiation.

ACKNOWLEDGMENTS

This research used the computational resources from the Stampede2 Startup allocation by the Extreme Science and Engineering Discovery Environment (XSEDE) program.

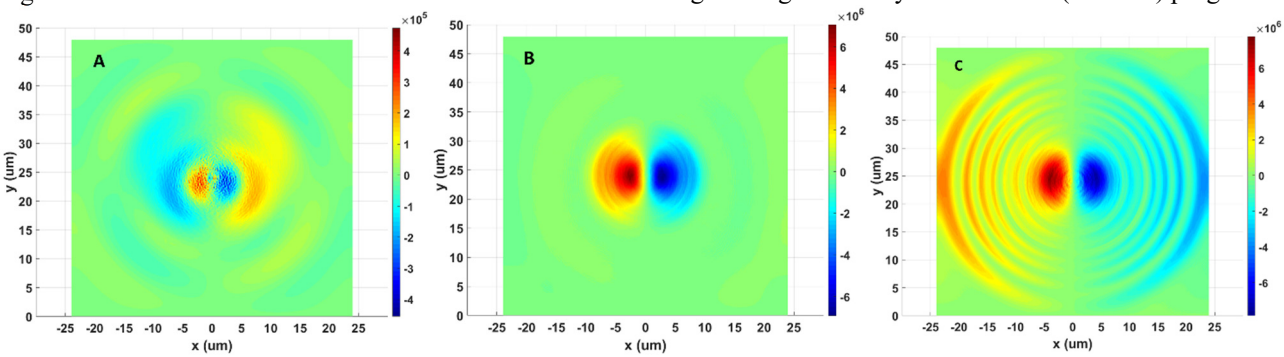

Figure 4: Crosssectional view of the laser's induced field propagation. A) Laser's induced fields interaction prior to collision. B) Plasma dipole formation. C) Transversal radiation wavefronts emitted from induced dipole oscillations.

ISBN: 978-3-95450-223-3 ISSN: 2673-7000 doi:10.18429/JACoW-NAPAC2019-WEPLO18

REFERENCES

[1] K. Kwon *et al*., "High-Energy, Short-Duration Bursts of Coherent Terahertz Radiation from an Embedded Plasma Dipole," *Sci. Rep.*, vol. 8, 2018. doi:10.1038/s41598-017-18399-3

[2] R. Mankowsky *et al*., "Nonlinear lattice dynamics as a basis for enhanced superconductivity in YBa2Cu3O6.5," *Nature,* vol. 516, pp. 71–73, 2014. doi:10.1038/nature13875

[3] M. Först *et al*. "Nonlinear phononics as an ultrafast route to lattice control," *Nature Phys.,* vol. 7, pp. 854–856, 2011. doi:10.1038/nphys2055

[4] A. Dienst *et al*., "Bi-directional ultrafast electric-field gaing of interlayer charge transport in a cuprate superconductor," *Nature Photonics,* vol. 5, pp. 485–488, 2011. doi:10.1038/nphoton.2011.124

[5] E. Nanni *et al*., "Terahertz-driven linear electron acceleration," *Nature Comm*., vol. 5, p. 485, 2015. doi:10.1038/ncomms9486

[6] B. Williams *et al*., "High-power terahertz quantum-cascade lasers," *Elec. Lett.,* vol 42, pp. 89–91, 2006.

[7] C. Cheng *et al.,* "Generation of Electromagnetic Pulses from Plasma Channels Induced by Femtosecond Light Strings," *Phys. Rev Lett*., vol. 87, p. 213001, 2001.

[8] T. Tikhonchuk, "Comment on "Generation of Electromagnetic Pulses from Plasma Channels Induced by Femtosecond Light Strings," *Phys. Rev. Lett.* vol. 89, p. 209301, 2002.

[9] I. Thiele *et al*., "Theory of terahertz emission from femtosecond-laser-induced microplasmas," *Phys. Rev. E.,* vol. 94, p. 063202, 2016.

[10] H. Reid *et al.,* "A review of solar type III radio bursts," *Res. Astronomy and Astrophys.,* vol. 14, pp. 773–804, 2014.

[11] D. Melrose, "The emission mechanisms for solar radio bursts," *Space Sci., Rev.* vol. 26, pp. 3–38, 1980.

[12] T. Boyd, "Emission of Radio Noise by Plasmas," *Phys. Fluids,* vol. 7, pp. 59–63, 1964.

[13] P. Sturrock *et al*., "Radiation at the Plasma Frequency and its Harmonic from a Turbulent Plasma," *Phys. Fluids,* vol. 8, pp. 1509–1516, 1965.

[14] P. Yoon, "Plasma emission by a nonlinear beam instability," *Phys. Plasmas,* vol. 2, pp. 537–548, 1995.

[15] A. Benz "Millisecond Radio Spikes," *Solar Phys.,* vol. 104, pp. 99–110, 1986.

[16] W. Baumjohann and R. Treumann, *Basic Space Plasma Physics*. London, UK: College Press, 1996.

[17] G. Vieux *et al*., "An ultra-high gain and efficient amplifier based on Raman amplification in plasma." *Scientific Rep.,* vol. 7, p. 2399, 2017.

[18] H. Hamster *et al*., "Subpicosecond, Electromagnetic Pulses from Intense Laser-Plasma Interaction," *Phys. Rev. Lett.,* vol. 71, pp. 2725–2728, 1993.

[19] H. Hamster *et al*., "Short-pulse terahertz radiation from high-intensity-laser produced plasmas," *Phys. Rev. E.,* vol. 49, pp. 671–677, 1994.

[20] U. Teubner *et al*., "Observation of VUV radiation at wavelengths in the $\omega p-$ and $2\omega p-$wavelength range emitted from femtosecond laser-plasmas," *Opt. Comm.,* vol. 144, pp. 217–221, 1997.

[21] A. Proulx *et al*., "Fast pulsed electric field created from the self-generated filament of a femtosecond Ti:Sapphire laser pulse in air," *Opt. Comm.,* vol. 174, pp. 305–309, 2000.

[22] C. Chin-Fatt *et al*., "Enhanced Radiation from a Theta-Pinch Plasma," *Phys. Rev. Lett.* vol. 25, p. 1644, 1970.

[23] J. Kim *et al*., "Relativistic terahertz pulse generation by nonlinear interaction of a high-power fs laser with underdense plasmas," *J. Phys. D: Appl. Phys.,* vol. 45, p. 395201, 2012.

[24] K.Yee, "Numerical solution of initial boundary value problems involving Maxwell's equations in isotropic media," *IEEE Trans. Antennas Propag*., vol. 14, pp. 302-307, 1966.

[25] K. Yu and V. Samulyak, "SPACE code for beam-plasma interaction", in *Proc. 6th Int. Particle Accelerator Conf. (IPAC'15)*, Richmond, VA, USA, May 2015, pp. 728-730, doi:10.18429/JACoW-IPAC2015-MOPMN012

[26] K. Yu *et al*., "Simulation of beam induced plasma in gas-filled rf cavities," *Phys. Rev. Accel. Beams*, vol. 20, p. 032002, 2017.

[27] K. Yu *et al*., "Simulation of plasma loading of high-pressure RF cavities," *Journal of Instrumentation*, vol. 13, 2018.

[28] K. Yu, M. Chung, A. V. Tollestrup, K. Yonehara, B. T. Freemire, and V. Samulyak, "Modeling and Simulation of Beam-induced Plasma in Muon Cooling Devices", in *Proc. 5th Int. Particle Accelerator Conf. (IPAC'14)*, Dresden, Germany, Jun. 2014, pp. 466-468. doi:10.18429/JACoW-IPAC2014-MOPME043

[29] J. Ma *et al*., "Simulation studies of modulator for coherent electron cooling," *Phys. Rev. Accel. Beams*, vol. 21, p. 111001, 2018.

[30] J. Ma, V. Samulyak, K. Yu, V. Litvinenko, and G. Wang, "Simulation of Beam-Induced Plasma for the Mitigation of Beam-Beam Effects", in *Proc. 6th Int. Particle Accelerator Conf. (IPAC'15)*, Richmond, VA, USA, May 2015, pp. 734-736. doi:10.18429/JACoW-IPAC2015-MOPMN015

[31] P. Kumar *et al*., "Simulation study of CO2 laser-plasma interactions and self-modulated wakefield acceleration," *Phys. Plasmas*, vol. 26, p. 083106, 2019.

[32] P. Kumar, K. Yu and R. Samulyak, "Influence of ionization and beam quality on interaction of TW-peak CO2 laser with hydrogen plasma," *J. Phys*., vol. 1067, p. 042008, 2018.